

ROOFTOP AND GROUND STANDARD
TEMPERATURES: A COMPARISON
OF PHYSICAL DIFFERENCES

Brian D. Griffith
Thomas B. McKee

LIBRARIES

AUG 31 2000

COLORADO STATE UNIVERSITY

**Colorado
State**
University

Climatology Report No. 00-2

**DEPARTMENT OF
ATMOSPHERIC SCIENCE**

PAPER NO. **694**

ROOFTOP AND GROUND STANDARD TEMPERATURES:
A COMPARISON OF PHYSICAL DIFFERENCES

Brian D. Griffith

Thomas B. McKee

This research was supported by NOAA,
National Weather Service, Office of
Meteorology, under grant
NA67RJ0152 Amend 21.

Atmospheric Science Department
Colorado State University
Fort Collins, CO 80523-1371

July 2000

Atmospheric Science Paper # 694

Climatology Report No. 00-2



018401 9741150

Abstract

ROOFTOP AND GROUND STANDARD TEMPERATURES: A COMPARISON OF PHYSICAL DIFFERENCES

Accuracy and continuity of surface air temperature measurements are critical for many meteorological activities including short-term weather forecasting, warnings, and climate monitoring. In the United States and worldwide, most air temperature observations have historically been taken at a height of approximately 1.25 to 1.5 meters above the ground over a grass surface. In the last two decades, there has been a rapid expansion of nonfederal weather station networks to support state, regional and community needs. Many of these new weather stations are located on rooftops for reasons of security or convenience. Mixing these rooftop observations indiscriminately with observations from standard screen-height can pose significant issues for weather forecasting and verification, weather and climate analysis and climate applications such as energy demand planning and forecasting by large public utilities. This study establishes the physical mechanisms which cause a rooftop sensor to have a temperature bias relative to a nearby ground sensor. From a surface energy balance perspective, the physical characteristics of a surface are analyzed and related to temperature bias. This study identifies the surfaces and conditions leading to rooftop temperature bias in both maximum and minimum temperatures. These concepts are verified through both surface radiating temperature measurements and air temperature measurements contrasting roof

and ground temperatures. Guidelines are then proposed to establish which roofs are unsuitable for temperature measurements and under what conditions a rooftop is vulnerable to temperature bias.

Results indicate that overcast skies lead to small rooftop to ground differences in both surface radiating temperature and air temperature. Observations show differences of approximately 1°C or less in radiating temperature and less than 1°C in air temperature. An exception was observed where a wall effect led to more than a 2°C difference in air temperatures between roof and ground.

Clear or partly cloudy skies allow larger rooftop temperature biases to develop. Roof to ground differences in surface radiating temperatures of up to 30°C were observed. Although air temperature measurements were not made at all locations, observations show roof to ground differences of 3°C for radiating temperature differences of 14°C. The potential for even greater roof-ground air temperature differences exists at sites where radiating temperatures are further apart.

ACKNOWLEDGEMENTS

The authors would like to thank the members of the research group for their assistance: Odie Bliss for her endless help with all logistical and administrative aspects; John Kleist who provided support for all computer-related issues; Nolan Doesken for his helpful comments and insights; and Chris Castro for helping clarify ideas and for proofing multiple drafts.

Additional thanks are extended to John Davis for his help with the pyrgeometer and for helping to determine field of view for the KT19, and to Bob Stone of NOAA for his assistance with the KT19 instrument.

Author Brian Griffith would like to extend a special thanks to his wife, Robyn, for everything.

This research was supported by the NOAA, National Weather Service, Office of Meteorology under grant NA67RJ0152 Amend 21.

TABLE OF CONTENTS

1. Introduction.....	1
1.1. Introduction.....	1
1.2. Exposure Standards	2
1.3. Proliferation of Rooftop Sensors	2
1.4. Variability of Rooftop Exposures.....	3
1.5. Potential Impacts of Rooftop Exposures	3
1.6. Previous Studies of Rooftop Exposures	4
1.7. Goals of the Study	6
2. Methodology	7
2.1. Theoretical Model of the Surface Energy Budget.....	7
2.2. Contribution of Surface Characteristics.....	14
2.3. Contribution of Non-Surface Characteristics	17
2.4. Factors Contributing to Rooftop Bias.....	19
2.5. Data Collection	24
3. Results.....	27
3.1. Cloudy Sky Cases	27
3.1.1. Radiation Measurements.....	27
3.1.2. Air Temperature Measurements	28

3.2. Clear Sky Cases	33
3.2.1. Radiation Measurements.....	34
3.2.2. Air Temperature Measurements	35
4. Conclusions.....	46
5. References.....	48

LIST OF TABLES

1. Previous Studies of Roof-Ground Temperature Bias	6
2. Albedos of Representative Surfaces	15
3. Emissivities of Representative Surfaces	15
4. Representative Values of Thermal Conductivity	16
5. Effect of Sky View Restriction	18
6. Factors Contributing to Rooftop Temperature Bias.....	24
7. Surface Radiating Temperature Measurements for Cloudy Cases	28
8. Surface Radiating Temperature Measurements for Clear Cases	34

LIST OF FIGURES

1. Energy Balance Components.....	8
2. Radiation Budget Components	9
3. Relationship Between Surface Temperature and Surface Energy Flux.....	12
4. Pyrgeometer Surface Radiating Temperatures vs. Air Temperatures	12
5. Common Sky-View Restrictions	18
6. Crest Hill Temperatures.....	30
7. Crest Hill Differences	30
8. CSU Wall Effect Temperatures	32
9. CSU Wall Effect Temperature Differences	32
10. Blevins Morning Temperatures.....	37
11. Blevins Morning Differences	37
12. Blevins Afternoon Temperatures	38
13. Blevins Afternoon Differences.....	38
14. Cody Temperatures	41
15. Cody Differences.....	41
16. Department Series One Temperatures.....	44
17. Department Series One Differences	44

INTRODUCTION

1.1 Introduction

Accuracy and continuity of surface air temperature measurements are critical for many meteorological activities including short-term weather forecasting, warnings, and climate monitoring. In addition, surface air temperature records are widely used by the private sector for activities such as energy demand planning and the public sector through media forecast outlets. Surface air temperature is probably the most publicly familiar and widely used meteorological variable.

In the United States, there are two official national observing networks operated by the National Weather Service (NWS). The primary surface observing network is composed of the ASOS (Automated Surface Observing System) located mostly at a network of approximately 1000 airports (Leffler and Schiesl, 1994). In addition, the NWS Cooperative Observer Program provides about 5000 temperature sensors across the nation taking daily observations. While many of these co-op observations are not readily available to forecasters, they are incorporated into the national climate database at the National Climate Data Center (NCDC).

1.2 Exposure Standards

Historically, most air temperature observations have been taken over a grass surface at a height of approximately 1.5 meters above the ground. World Meteorological

Organization (WMO) rules for exposure call for the observed temperature to be representative of the free air conditions surrounding the station at a height of between 1.25 and 1.5 meters above ground level. The best site is over level ground and not shielded by or close to trees, buildings or other obstructions (WMO, 1996). The WMO also states that temperature observations on top of buildings are of doubtful significance due to vertical temperature gradient and the effect of the building itself on the temperature. NWS guidelines for instrument exposures are for the sensor to be located over ground that is typical of the surrounding environment. Additionally, temperature sensors should be installed in a position where they will not be influenced by obstructions in air circulation or by artificial construction such as extensive concrete or paved surfaces (NWS, 1972).

Rules for instrument exposures encourage consistent and uniform observations that are accurate and representative of the air temperature where people live, work, play and grow their food. Standardization of instrument exposures is essential for normalizing climate data collection and monitoring climate.

1.3 Proliferation of Rooftop Sensors

However, in the last twenty years, there has been an explosion of nonfederal weather station networks to support regional and community needs (Meyer and Hubbard, 1992). Often, the networks are based in schools and are supplied or sponsored by the local news media. Most of these networks consist of commercial off-the-shelf instrument packages with exposure and installation guidelines provided by the manufacturer. As a result, many of them are located on rooftops. Rooftop sites are attractive in urban areas for many reasons including the lack of a nearby ground based site, security from

vandalism, and convenience. In many cases these non-federal networks provide real-time data access through the internet and widespread public dissemination by the media. In forecast zones with a low density of readily available ‘official’ observations, these non-standard instruments may provide the majority of observational data for NWS or media forecasters.

1.4 Variability of Rooftop Exposures

Since non-standard instruments are often installed by the end-user, there exists a wide variety of exposures among rooftop sites. First, there are large inconsistencies in roof design. Design features with potential impacts to instrument siting include the pitch of the roof, the roof material, obstructions on the roof, multiple roof levels, retaining walls or a parapet around the edge of the roof, and ventilation system exhaust outlets. An example of a common manufacturer-recommended guideline is to install the temperature sensor on a rooftop away from obstructions and on the side of the roof facing the prevailing wind to minimize the fetch over the roof (AWS, 1998). AWS recommends the instrument to be located some distance above the roof surface on a pole mounted to an exterior wall. However, instruments from other manufacturers seen during this study were mounted in all sorts of locations, from less than one meter above a steeply pitched metal roof to located inside a wooden box located within one meter of an exhaust vent. There is a wide variability among instrument exposures.

1.5 Potential Impacts of Rooftop Exposures

Mixing rooftop observations indiscriminately with observations from standard screen height can pose significant issues for weather forecasting and verification, weather

and climate analysis and important applications such as energy demand planning and forecasting by large public utilities. Many data users are not aware of the potential impacts associated with rooftop observations. In addition, some rooftop data are included in National Oceanic and Atmospheric Administration/National Climate Data Center climate data sets without any obvious flags alerting data users to this fact. Threshold based forecasting can be severely impacted by unknowing use of rooftop temperatures. For instance, if a rooftop temperature has a 5 °C warm bias on a wet morning such that the sensor reads 3 °C while the free air temperature is two degrees below freezing; the forecaster will miss the warning for icy conditions. Climatologies that include biased rooftop temperatures will not be representative of true air temperatures and, if used for planning purposes, may cost money when the recorded conditions are only realized on top of a roof and nowhere else. Additionally, if a station moves from a ground site to a roof site and the record is not flagged, the data may suffer from a rooftop warm bias. If the bias is seasonal and weather dependent, it may be difficult to detect by casual analysis of the record.

1.6 Previous Studies of Rooftop Exposures

While weather stations on rooftops have existed for quite some time, there have been few efforts to quantify any bias they might have from standard ground stations. Laskowski (1936) reviewed the temperature records for an instrument on the roof of the Federal Building in Topeka, KS, from 1924 – 1934. He found that the mean temperature for the entire period was 13.2 °C on the roof. The ground exposure average temperature was 13.6 °C. The mean maximum temperatures on the roof averaged 0.94 °C cooler than

the ground while the mean minimum temperatures on the roof averaged 0.28 °C warmer than the ground.

Robb (1937) studied two years of observations at the Topeka site and compared roof to ground temperatures. He found that while the monthly mean temperatures were almost identical that the roof was cooler than the ground in the monthly mean maximums and the roof was warmer than the ground in the monthly mean minimums. Robb noted that four elements affected the difference between the maxima at the exposures: present weather, wind direction, wind speed and ground moisture.

Leffler and Schiesl (1994) studied two rooftop sites versus two ground standard sites for the time of January – August 1994 in North-Central Maryland. They discovered monthly average maximum temperatures for the rooftop sites to be warmer than the ground sites in the spring and summer months up to a peak difference of 3.7 °C (maximum daily bias of 6.1 °C) in July. Monthly average minimum temperatures were also found to be warmer at the rooftop sites than the ground stations in the spring and summer months up to a peak difference of 2.4 °C (maximum daily bias of 3.9 °C) in July.

Armstrong (1974) observed a rooftop instrument to produce cooler temperatures in the maximum than a nearby ground site in Southampton, U. K., with the smallest differences in the winter. However, he states that the roof was warmer than the ground station in the minimum temperatures. He also observed a distinct seasonal pattern such that the roof-ground difference in the maximum temperatures (roof cool bias) increased from winter to summer and that the roof-ground difference in the minimum (roof warm bias) increased from summer to winter. The largest mean differences Armstrong observed were only up to 0.6 °C. The results of these previous studies are summarized in Table 1.

Table 1. Previous studies of average roof-ground temperature bias (degrees C).

Study	T Max (Summer)	T Min (Summer)	T Max (Winter)	T Min (Winter)
Laskowski (annual mean)	-0.94	0.28		
Robb (daily)	up to -3.3	up to 7.2		
Leffler Schiesl (mean monthly)	3.7	2.4	0.1	-0.4
Armstrong (3 year mean)	-0.87	0.47	-0.13	0.70

1.7 Goals of this Study

This study is an effort to establish the relationship between rooftop and ground-standard temperature observations. The goal of the study is to determine the physical causative mechanisms leading to rooftop temperature bias under different seasonal and synoptic conditions by first developing a theoretical model of the energy interactions between a surface and the lowest layer of air. This model will provide a framework to observe which surface and non-surface characteristics contribute to the forcing of the air temperature. After identifying those characteristics, the study will propose how and under what conditions a roof might have a large temperature bias, both day and night. Through an understanding of the physical processes contributing to bias in rooftop temperatures, this study will attempt to identify which roofs are representative under which conditions and which roofs are unsuitable for air temperature measurements.

METHODOLOGY

2.1 Theoretical Model of the Surface Energy Budget

The following discussion of the energy budget is modified from Oke (1978) and Carlson et al. (1981). The basic energy balance of a surface with no heat storage can be written as:

$$Q^* = QG + QE + QH \quad (1)$$

where QG is the ground heat flux, QE is the evaporative or latent heat flux and QH is the sensible heat flux. The sign and magnitude of Q* (net radiation) force the right hand side of eq. 1. Figure 1 shows the diurnal variation of each variable in eq. 1.

From equation 1, Q* is the net radiation at the surface and can be expressed as:

$$Q^* = K\downarrow - K\uparrow + L\downarrow - L\uparrow \quad (2)$$

$K\downarrow$ is incoming solar radiation, $K\uparrow$ is reflected solar radiation, $L\downarrow$ is incoming longwave radiation and $L\uparrow$ is outgoing longwave radiation. Net radiation is typically large and positive during the day and small and negative at night. A typical summertime diurnal cycle of each variable in eq. 2 is shown in Figure 2.

Using the Stefan-Boltzmann equation for emitted longwave and Kirchoff's Law for reflected longwave when $\varepsilon \neq 1$, net longwave radiation can be written as:

$$L\downarrow - L\uparrow = L\downarrow - (1-\varepsilon)L\downarrow - \varepsilon\sigma T_s^4 \quad (3)$$

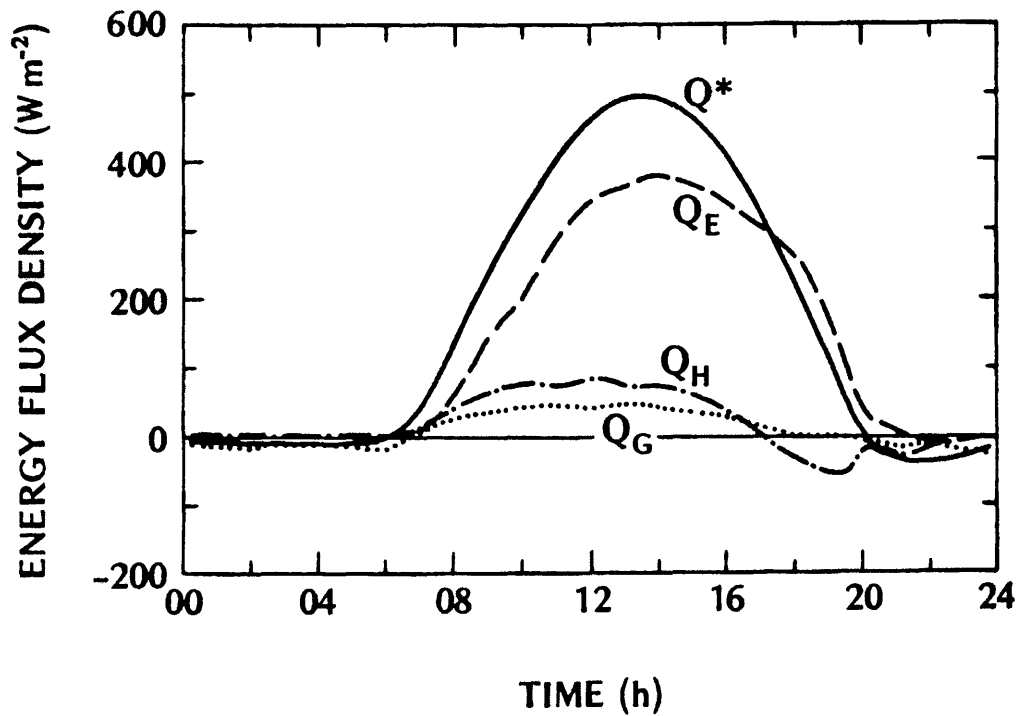


Figure 1. Energy balance components through the diurnal cycle. From Oke, 1978.

ϵ is the emissivity of the surface and T_s is the temperature of the surface. If net solar radiation flux at the surface ($K\downarrow - K\uparrow$) is written in terms of the surface albedo (A_s) and the solar radiation incident on the surface (S), then the net radiation can be written as:

$$Q^* = (1 - A_s)S + \epsilon L\downarrow - \epsilon\sigma T_s^4 \quad (4)$$

Thus, the left-hand side of eq. 1 is written in terms of incoming solar and longwave radiation and the characteristics of the surface (A_s , ϵ , T_s).

The right-hand side of the energy balance can be broken into components as well.

The ground heat flux can be written as:

$$Q_G = -\lambda \Delta T / \Delta z_g \quad (5)$$

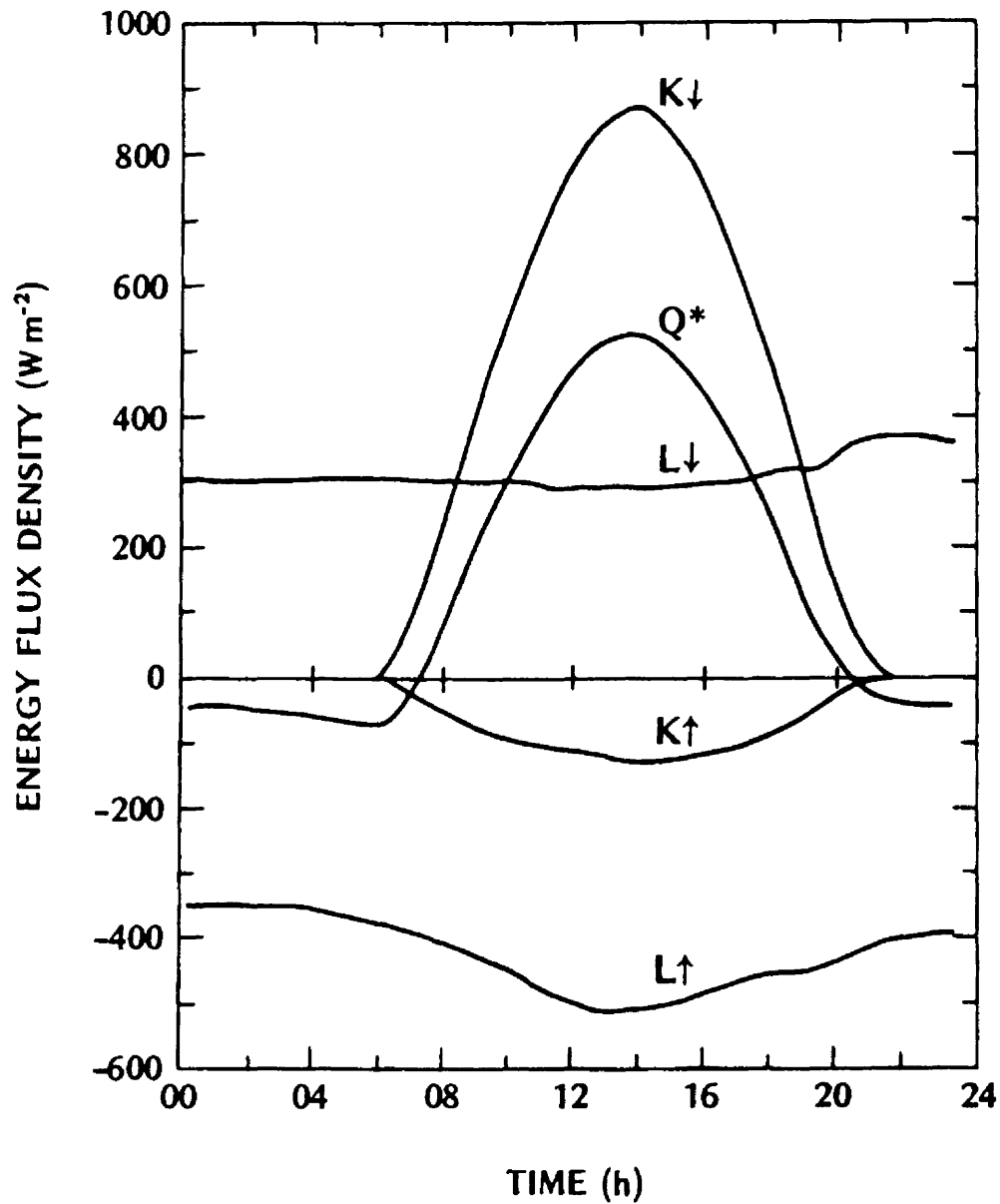


Figure 2. Radiation budget components through the diurnal cycle. From Oke, 1978.

where λ is the thermal conductivity ($\text{Wm}^{-1}\text{K}^{-1}$) and $\Delta T/\Delta z_g$ is the vertical temperature gradient from the surface into the ground. By day, $\Delta T/\Delta z_g$ is negative, as the temperature is cooler beneath the surface. Thus, during the day, QG is positive and represents an energy flux downward from the surface.

The surface flux of sensible heat can be written as:

$$QH = -\rho c_p K_H (\Delta T / \Delta z_a) \quad (6)$$

where c_p is the specific heat of air at constant pressure, K_H is the eddy diffusivity, and $\Delta T / \Delta z_a$ is the thermal gradient from the surface to the air.

Latent heat flux (QE) can be written as:

$$QE = -\rho L_v K_w \Delta q / \Delta z \quad (7)$$

where ρ is air density, L_v is the latent heat of vaporization, K_w is the eddy diffusivity of water vapor and $\Delta q / \Delta z$ is the gradient of water vapor from the surface through the layer of air.

The Bowen ratio is a measure of how much surface energy is used for sensible heat versus latent heat and is expressed:

$$B = QH / QE \quad (8)$$

For a given amount of surface energy, a Bowen ratio of one indicates an equal amount of energy channeled into sensible heating of the atmosphere and evaporation of surface moisture. A Bowen ratio less than one indicates more available surface energy is going to evaporation and less to sensible heating of the air.

Combining eqs. (1) and (4) and substituting for the explicit energy flux terms, the total energy balance of a surface can be written as:

$$(1 - A_s)S + \epsilon L \downarrow - \epsilon \sigma T_s^4 = -\lambda \Delta T / \Delta z_g - \rho c_p K_H (\Delta T / \Delta z_a) - \rho L_v K_w \Delta q / \Delta z \quad (9)$$

Now, consider an air volume or parcel such that the ground surface forms the lower boundary of the volume. From the first law of thermodynamics:

$$dQ = c_p dT \quad (10)$$

Thus, the temperature of a volume of air near the ground can change as a result of a change in energy of the parcel.

Consider the time rate of change of temperature of an air parcel. The total derivative DT/Dt may be expanded to be written as:

$$DT/Dt = \delta T/\delta t + (u\delta T/\delta x + v\delta T/\delta y + w\delta T/\delta z) \quad (11)$$

where $\delta T/\delta t$ is the local time rate of change of temperature while $(u\delta T/\delta x + v\delta T/\delta y + w\delta T/\delta z)$ is the time rate of change of temperature moving with the parcel, or advection. Advection is the transport of air from surrounding environments to the environment being sampled. Advection can bring warmer, cooler, wetter or drier air into the sample space. However if winds are light (u and v close to zero), horizontal advection can be neglected. Then only radiative and sensible heat flux will effect temperature change.

During the day, when the left-hand side of eq. 9 is positive, a portion of the available Q^* (the percentage of which is related by the Bowen ratio) will be transferred into the air by sensible heating (QH). At night, when Q^* is negative and the air-ground temperature gradient reverses, there will be an energy flux from the air volume as sensible heat is transferred from the air into the ground. In general, the points where Q^* equals zero are the times of maximum and minimum temperature (See Figure 3). Thus, the surface sensible heat flux is the primary determinant of the air temperature of the lowest layer of the atmosphere over an ideal site (neglecting advection).

If the air temperature of a layer over a surface is driven by the surface sensible heat flux, then the temperature of the surface is of primary importance. The variation of surface temperature affects the magnitude and the sign of the temperature gradient

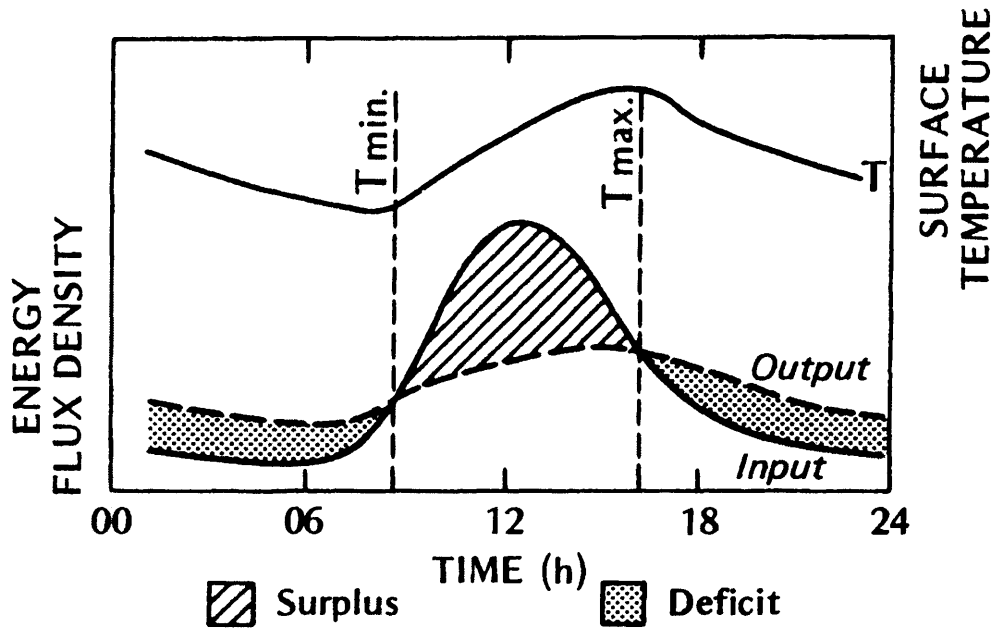


Figure 3. Relationship between surface temperature and surface energy flux where $Output = K\uparrow + L\uparrow$, $Input = K\downarrow + L\downarrow$, and $Q^* = Input - Output$. From Oke, 1978.

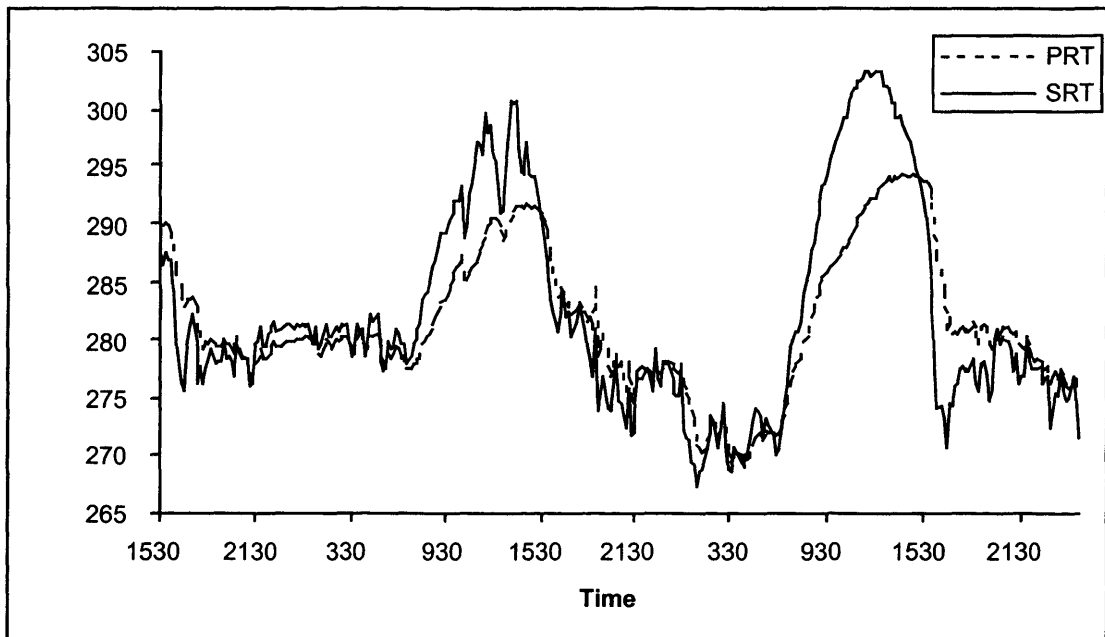


Figure 4. Pyrgometer readings of surface radiating temperature vs. PRT measurements of air temperature 1.5m above the surface at Platteville, CO.

$\Delta T/\Delta z_g$ and $\Delta T/\Delta z_a$ thus driving the energy fluxes on the right hand side of eq. 9. Figure 4 shows the relationship between surface temperature and air temperature on a fall day in Colorado. In other words, given a set of solar and downward longwave conditions (S and $L\downarrow$, eq. 9) and knowledge of surface moisture values, a measurement of surface temperature should indicate the magnitude of sensible heat flux taking place.

The relationship of air temperature to the surface radiating temperature can be shown in a simplified way by assuming a dry surface and using a finite difference form of the temperature gradients to express eq. 9 as:

$$T_a = T_s - [z_a/(\rho c_p K_h)] * [(1-A_s) + \epsilon L\downarrow - \epsilon \sigma T_s^4 + \lambda(T_s - T_g)/z_g] \quad (12)$$

where T_a is air temperature at height z_a and T_g is ground temperature at depth z_g . A reasonable set of values for a grass lawn on a summer day could include: $A_s = 0.26$, $\epsilon L\downarrow = 0.97$, $\lambda = 0.25 \text{ Wm}^{-1}\text{K}^{-1}$, $\rho = 1.2 \text{ Kgm}^{-3}$, $c_p = 1005 \text{ JKg}^{-1}\text{K}$, $\sigma = 5.67 \times 10^{-8} \text{ Wm}^{-2}\text{K}^{-4}$, $T_g = 308 \text{ K}$, $z_a = 2 \text{ m}$, $z_g = 0.1 \text{ m}$. For these example values and a surface temperature of 323 K , $T_a = 298.7 \text{ K}$ from eq. 12. This air temperature is $24.3 \text{ }^\circ\text{C}$ less than the surface temperature. The sensitivity of the air temperature to the surface temperature can be seen if surface temperature is then assumed to be somewhat cooler at 310 K . For $T_s = 310 \text{ K}$, the air temperature is 278.8 K , which is $31.2 \text{ }^\circ\text{C}$ less than the surface temperature. Note that while the air temperature has decreased with decreasing surface temperature, the gradient ($T_a - T_s$) has increased. Eq. 12 reveals that, for a given set of solar conditions, if T_s is decreased then T_a changes in the same direction. However, when the surface temperature decreases then the upwelling longwave radiation is less. There is increased net radiation as a result. The temperature difference between the surface and the ground at depth z_g will be less, decreasing the ground energy flux (QG). This means that the

temperature difference ($T_a - T_s$) must get larger to increase the sensible heat flux, even though T_a decreases when T_s is decreased. This illustrates the feedback of T_s on the net radiation, ground heat flux, sensible heat flux and air temperature. The complex feedback between T_s and the other terms in eq. 9 allows the air temperature to change in the same direction as the surface temperature while the sensible heat flux changes in the opposite direction. Additional complexities emerge when differences in moisture and ground conductivity are allowed. The reality is that the factors in eq. 9 of surface temperature, surface moisture, ground conductivity and emissivity together create a complex problem. Future research should include the development of a surface layer model to allow a more quantitative evaluation of the sensitivity of the energy balance to these terms.

When considering two distinct surfaces, surface temperature measurements should indicate how the sensible heat fluxes of the two surfaces compare and how air temperatures above the two surfaces compare. In order to compare two surfaces (e.g. roof and ground), examine the difference in the surface energy balance (eq. 9) by subtracting roof minus ground:

$$\begin{aligned}
 & -(\Delta A)S + \Delta \epsilon L \downarrow - \sigma(\epsilon_r T_r^4 - \epsilon_g T_g^4) = \\
 & \Delta(-\lambda \Delta T / \Delta z_g) - \Delta(\rho c_p K_H (\Delta T / \Delta z_a)) - \Delta(\rho L_v K_w \Delta q / \Delta z) \quad (13)
 \end{aligned}$$

2.2 Contribution of Surface Characteristics

From eq. 13, note the surface characteristics that contribute to different energy fluxes. Surface differences in albedo (A_s), emissivity (ϵ), and surface temperature (T) affect net radiation. Differences in thermal conductivity (λ), surface temperature (T), and surface moisture (q_s) affect the surface energy flux.

Table 2. Albedo of shortwave radiation for representative surfaces. From Pielke (1984).

Surface	A
Fresh snow	0.75-0.95
Clean old snow	0.55
Dirty old snow	0.45
Dark soil	0.05-0.15
Dry sandy soil	0.25-0.45
Dry concrete	0.17-0.27, 0.10-0.35
Road black top	0.05-0.10
Asphalt	0.05-0.20
Tar and gravel	0.08-0.18
Short grass (2cm)	0.16
Wet grass	0.20
Dry grass	0.30

Albedo estimates for various surfaces can be obtained and the difference then calculated for a specific roof versus ground site (see Table 2). Jones and Suckling (1983) found that the albedo for a conventional tar and gravel roof surface was about 0.10 while the albedo for a typical lawn was about 0.16. They found that this difference in albedo left the tar and gravel roof with more initial solar energy, which was then used for heating.

Table 3. Emissivities of longwave radiation for representative surfaces. From Pielke (1984).

Ground Cover	ϵ
Fresh snow	0.99
Old snow	0.82
Dry sand	0.96, 0.914
Wet sand	0.98, 0.936
Soils	0.90-0.98
Asphalt	0.95, 0.956
Concrete	0.71-0.90, 0.966
Tar and gravel	0.92
Limestone gravel	0.92
Grass lawn	0.97
Grass	0.90-0.95

The next variable in the surface energy balance is emissivity. Jones and Suckling (1983) found that the emissivity of a tar and gravel rooftop was approximately 0.02 to 0.03 lower than that of a nearby lawn surface. Arnfield (1982) found a range of urban emissivities to be 0.937 to 0.961 in snow-free conditions. These values are 0.01-0.03 lower than values for rural surfaces. If a rooftop surface has a lower emissivity than a ground surface, it loses less energy through longwave emission and reflects more downwelling longwave energy. The net effect of the difference in emissivity is that at high surface temperatures, the emissivity role is smaller. However, when the surface temperatures are lower, then the contributions to the energy balance from emissivity differences are significant.

Not only do urban-type surfaces have different emissivity and albedo properties than grass and soil, their subsurface heat storage is different. When the thermal conductivity of a surface changes, the surface will have a different ground energy flux. A surface with higher thermal conductivity will have more ground energy flux. This would leave less energy for sensible heating of the air.

Another factor in the contrast between rooftop and ground energy balance is surface moisture. Most rooftops (urban materials) will evaporate surface water rapidly

Table 4. Representative values of thermal conductivity for various types of surfaces. (Pielke, 1984).

Surface	λ (Wm ⁻¹ k ⁻¹)
Concrete	4.60
Rock	2.93
Snow	0.14, 0.08
Clay Soil (Dry)	0.25
Clay Soil (40% liquid water)	1.58
Sand Soil (Dry)	0.30
Sand Soil (40% liquid water)	2.20

and transition back to a 'dry' surface. These impervious dry surfaces transfer all of their available net radiation (Q^*) into sensible heat or ground heat fluxes in accord with the Bowen ratio. Considering that most roofs are well insulated, the ground flux (Q_G) term in the roof energy balance may be very small.

Irrigated lawns, however, channel their net radiation surplus into evaporation. Jones and Suckling (1983) found the temperature of a tar and gravel roof averaged 5-6 °C warmer than an adjacent irrigated lawn. The maximum measured daytime difference was 17 °C after lawn irrigation. In fact, evaporation can actually exceed net radiation by 5 percent over a 24 hour period (Oke, 1988). This is possible through the advection of hot dry air across the lawn from the surrounding dry surfaces. During this event, sensible heat flux could be negative while energy is transferred from the hot air to the cooler ground surface. Thus, for a dry roof and wet ground (lawn) site starting at the same surface radiating temperature, the lawn site will transfer less energy to warm the air above than the roof site.

2.3 Contribution of Non-Surface Characteristics

Sky-view factor is an important characteristic of the urban energy balance. A floor surface with no obstructions will radiate freely out to space. However, rooftop surfaces with obstructions or walls nearby may only see a partial clear sky hemisphere. For a point on the surface, the solid angle view of the clear sky is less (Figure 5). That is, an obstruction will replace a portion of the clear sky hemisphere and will radiate to the floor surface at a warmer temperature than the clear sky, decreasing the ability of the surface to cool.

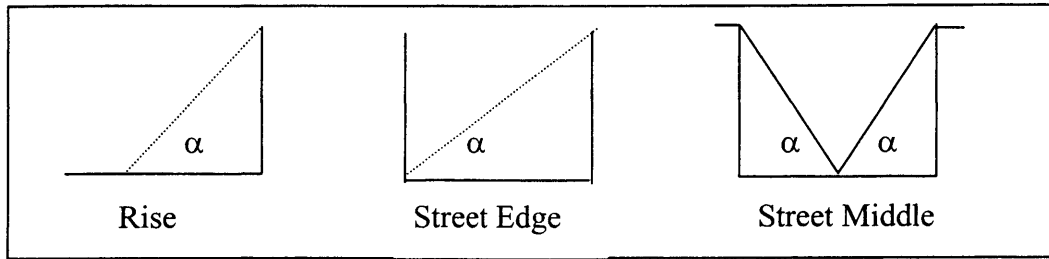


Figure 5. Common sky-view restrictions. Modified from Geiger, 1966.

Oke et al. (1991) modeled the temperature effects of restricted sky-view. A maximum effect of 5 °C warm bias over a 12-hour cooling period was found in a canyon geometry model with height/width ratio of 2.45:1 (Street Middle, $\alpha = 78.5$ degrees).

Geiger (1966) outlined the effective outgoing radiation from sheltered and inclined surfaces with varying sky-view factors (Table 5).

Table 5. Effect of sky-view restriction. The fractional amount of clear sky hemisphere seen by a point on a horizontal surface with restricted sky-view factor. Modified from Geiger, 1966.

Angle	0	5	10	15	20	30	45	60	75	90
Rise	1.0	0.997	0.992	0.988	0.979	0.951	0.877	0.772	0.639	0.50
Street Edge	1.0	0.930	0.862	0.797	0.737	0.622	0.452	0.296	0.143	0
Street Middle	1.0	0.993	0.984	0.976	0.958	0.902	0.754	0.544	0.279	0

Another possible consideration in the difference between rooftop and ground station observations derives from the variation of temperature with height above the ground. During the day, if the dry adiabatic lapse rate is considered, temperature would decrease 0.098 °C per ten meters.

Geiger (1966, Table 23) noted a seasonal and diurnal variation in average vertical temperature gradient in the layer from one meter to 15 meters. Nighttime $\Delta T/\Delta z_a$ peaked

in April at 0200hrs at $+0.84$ °C per 10 meters. Thus, a sensor at a rooftop height of approximately ten meters above ground could read 0.84 °C warmer than a ground-standard sensor at 1.5 meters. The median nighttime $\Delta T/\Delta z_a$ was 0.62 °C per ten meters during the time 2200 – 0200hrs.

Daytime lapse rates in the layer from one meter to 15 meters peaked at -0.63 °C per ten meters in August at 1200hrs. The median daytime lapse rate was -0.4 °C per ten meters during the time 1000–1400hrs.

Note, however, that the temperature variations with height attributed to these lapse rates are in the free air and do not consider the surface energy budget of the rooftop itself. The extreme lapse rates could only be brought about by calm, windless conditions that minimize the mixing of the air closest to the ground. These windless conditions will maximize the rooftop surface energy contributions to the temperature of the air sampled by a rooftop sensor. Such conditions reduce the possibility of the sensor sampling the advection of free air characterized by these extreme lapse rates. Hence, temperature differences between roof and ground due to vertical temperature gradients over ten to twenty meter heights are on the order of 1 °C.

The surface energy flux is the dominant contributor to the air temperature observed by a sensor at both rooftop and screen heights. Lapse rates alone are not likely to contribute to large temperature bias between roof and ground temperatures except in the case where the ground sensor itself is located in an unrepresentative site such as a depression where cold air can pool during the night.

2.4 Factors Contributing to Rooftop Bias

From the previous survey of the difference between the energy balance of two surfaces, eq. (13), a list of rooftop temperature forcing factors and their possible magnitudes can be made.

1. **Inversion/Lapse Rate:** The daytime lapse rate could account for a maximum difference of about 0.4 °C per ten meters difference in height for typical rooftop heights. The evening $\Delta T/\Delta z_a$ could produce a maximum difference of about 0.6 °C per ten meters. Note, however, that the calm conditions contributing to strong lapse rates impede the advection of lapse-modified air to sensors located on a rooftop.
2. **Thermal Conductivity of Materials:** When thermal conductivity varies between surface materials, they will have different ground energy fluxes (QG) For a surface material with a large ground conductivity, the ground energy flux may be higher, thus reducing the energy available for sensible heating of the air.
3. **Bowen Ratio of Roof Materials v. Ground:** Most rooftops will evaporate any surface water rapidly and transition back to a 'dry' surface. These impervious dry surfaces transfer all of their positive net radiation (Q^*) into sensible heat to warm the air above or the substrate below. Irrigated lawns, however, channel their available energy into evaporation instead of sensible heating of the air. Jones and Suckling (1983) found the temperature of a tar and gravel roof to average 5 to 6 °C warmer than an adjacent irrigated lawn surface with a maximum measured daytime difference of 17 °C after lawn irrigation.

4. Rooftop Exhaust: Anthropogenic sources of heat on rooftops are common. Heating, ventilation and air conditioning exhaust, kitchen exhaust and other heat sources are easily detected and must be avoided.
5. Albedo: Jones and Suckling (1983) found that the albedo for a conventional tar and gravel roof surface was about 0.10 while the albedo for a typical lawn was about 0.16. This difference in albedo left the tar and gravel roof with more initial solar energy, which was then used for heating the air above.
6. Emissivity: The Stefan-Boltzmann law shows that the emissivity (ϵ) of the surface and the temperature of the surface determine the outgoing portion of the longwave radiation balance (eq. 3). Jones and Suckling (1983) found the emissivity of a tar and gravel rooftop was approximately 0.02 – 0.03 lower than that of a nearby lawn surface. A surface with lower emissivity will lose less energy to longwave emission and thus stay warmer (more positive Q^*).
7. Sky View: Obstructions in the sky-view of a floor surface alter the exchange of radiation between the sky and the surface. For a point on a horizontal surface, an obstruction replaces part of the cold sky hemisphere with a much warmer surface that radiates to the floor surface, decreasing the ability of the surface to cool.
8. Wall Effect: A combination of heat capacity, anthropogenic heat sources and sky view contributes to make vertical walls significantly warmer than other surfaces. Particularly in the winter, low sun angles can deliver more direct solar radiation to vertical walls than horizontal surfaces. As the walls are heated relative to the environment, the air in close proximity to the wall warms and rises up the wall. Rooftop temperature sensors mounted directly above the wall are then bathed in a

plume of rising warm air. In addition, vertical walls typically have less insulation than roofs and are able to transmit heat through windows contributing to make vertical walls particularly warm in winter.

Analyzing eqs. 9 and 13, the factors which result in a roof having a warm, neutral or cold bias can be determined (Table 6). There are certain conditions that contribute to daytime warm temperature bias. Roofs with a low albedo absorb more solar radiation (Q^*) and warm during the day. They will have more available Q^* to be used for heating. Roofs with a restricted sky view will have an increase in $L\downarrow$ and thus more available Q^* . Rooftop surfaces that are dry or will dry quickly due to water runoff, have a lack of evaporation relative to a lawn-type ground surface. A dry roof will have less Q_E and thus more energy available for Q_H . In addition, well insulated roofs that have a low conductivity will have less ground heat flux (Q_G) and will be able to channel more energy into sensible heating of the atmosphere. Finally, sensors mounted on or above south or west facing walls may be bathed in a rising plume of warm air resulting in anomalously warm rooftop temperatures

Setting incoming solar (S) to zero in eq. 9 identifies the factors leading to a warm roof overnight. As the left hand side of eq. 9 becomes negative it is evident that stored solar energy in the ground could yield a large $\Delta T/\Delta z_g$ and thus a large negative Q_G , or flux from the ground to the surface. This source of energy to balance the negative Q^* could warm the surface and thus slow the sensible heat flux from the air to the surface. Heat exhaust on the roof could artificially warm the roof environment relative to the ground. If the roof surface radiating temperature is high then Q_H could remain positive or

less negative. In other words, if the surface remains warm then it can still heat the cooler air above or at least minimize the energy flux from the air to the surface if the air is warmer than the surface. Finally, background atmospheric vertical temperature gradients could result in the air at rooftop level being warmer than the air at ground level.

There are two cases that force a roof neutral or the same temperature as the ground surface. The first case is an overcast sky or clouds that reduce downwelling solar (S), and increase L_{\downarrow} such that Q^* is small. When Q^* is small the energy fluxes on the right hand side of eq. 9 are also small and no large differences between roof and ground can develop.

The second case that will force a roof to be neutral is strong advection. If the wind is blowing strongly, then the local air temperature no longer depends on local surface conditions and is instead a characteristic of the advected air, i.e. the temperature of the air is determined upstream.

A roof could be cold relative to a ground surface if the characteristics for a warm roof are reversed. During the day, if a rooftop has a high albedo it will reduce the Q^* available for heating. If the rooftop is wet then available Q^* will be directed to Q_E instead of Q_H . High rooftop conductivity results in large Q_G and thus less Q_H . Additionally, daytime lapse rates result in temperatures at rooftop height being less than at the ground surface. Finally, the only way a roof could be cold in the minimum temperatures is to have a low surface temperature such that the air above is warm relative to the roof resulting in a sensible heat flux from the air to the surface.

Table 6. Factors contributing to rooftop temperature bias

Roof Bias	T Max	T Min
Roof warm	Low albedo (increased Q^*) Sky view (increased L_{\downarrow}) Lack of evaporation (small QE) Low ground conductivity (small QG) Wall mount	Stored solar energy in ground (negative QG) Heat exhaust Roof SRT high (large QH) Wall mount Atmospheric dT/dz
Roof neutral	Clouds Advection	Clouds Advection
Roof cold	High albedo (decreased Q^*) Evaporation (large QE) High ground conductivity (large QG) Atmospheric dT/dz	Roof SRT low (negative QH)

2.5 Data Collection

Data collection involved two different measurements. First, using calibrated aspirated temperature sensors, air temperatures were sampled both on the roof and on the ground at subject sites. Second, an infrared radiometer recorded the surface radiating temperatures of dominant surfaces in the environment surrounding the temperature sensors. The infrared radiometer measures the incident longwave radiation from a certain field of view and then computes the surface radiating temperature based on a user specified emissivity (ϵ).

A RM Young platinum resistance thermometer (PRT) was used to sample air temperature. The platinum resistance thermometer was housed in a RM Young 43408 Aspirated Radiation Shield. The PRT was connected to a CR10 or CR10X datalogger through a full-bridge circuit. The datalogger sampled and recorded the output voltage and transformed the voltage into a temperature value through a least squares polynomial calibration curve. The instruments were calibrated at the National Center for Atmospheric

Research Foothills Laboratory in a silicon bath with calibration points at ten degree C intervals from $-40\text{ }^{\circ}\text{C}$ to $+30\text{ }^{\circ}\text{C}$. The three separate PRTs used in the study were calibrated to within $0.01\text{ }^{\circ}\text{C}$.

Two different infrared thermometers served to measure surface radiating temperatures. The first instrument was a Heimann KT19 Radiation Pyrometer connected to a CR10X datalogger. The second instrument was a Cole-Parmer Infrared Thermometer. While emissivity values for the surfaces of interest vary from 0.90 to 0.99, both sensors used an emissivity of 0.98 in their calculations of measured radiation to surface radiating temperature. According to the Stefan-Boltzmann law, for a given amount of measured radiation, a higher emissivity will yield a lower surface radiating temperature. By specifying the emissivity at the high end of the range of interest, the instrument will return conservatively lower SRTs than if a lesser emissivity was used in the calculations. A field calibration proved the two infrared radiometers to be within 0.1 degree C of each other.

There were two phases of rooftop temperature observations. In all locations, the infrared radiometer was used to measure SRTs of roof and ground surfaces. Around the time of maximum and minimum temperatures, radiation measurements were taken to compare the surface radiating temperatures of roof and ground and to determine what differences exist between various surfaces. In addition, SRT measurements were often made of walls, nearby parking lots, and any other surfaces in the area for comparison and reference.

In certain locations, a PRT sensor was established next to the present rooftop sensor to record air temperatures on the roof. The rooftop PRT ran for the duration of the

observation period. In addition, ground-based PRTs were set up to sample air temperatures representative of standard screen height measurements when a suitable ground location was available. The PRTs were mounted on tripods at a height of approximately two meters above the surface. At most sites, security considerations restricted the ground observation period to the early morning (daily minimum temperature) and afternoon (daily maximum temperature). However, at some locations, the ground instruments could safely run unattended for the entire period and gather data for the complete diurnal cycle.

A comparison of surface radiating temperatures with PRT air temperatures was used to determine what role surface radiating temperatures play in the differences between rooftop and ground air temperature measurements.

RESULTS

3.1 Cloudy Sky Cases

The first set of results is for cases where the skies were overcast at the time of observation. The overcast ceiling should lead to small net radiation (Q^*) by reducing the incoming solar and increasing the incoming longwave radiation. The small net radiation should, in turn, lead to small sensible heat fluxes and thus small differences in surface and air temperatures.

3.1.1 Radiation measurements

Radiation measurements from multiple sites indicate that surface radiating temperature differences are small when skies are overcast. In most cases observed in this study, surface radiating temperature differences between roof and ground were less than one degree C during overcast periods. Table 7 summarizes the results of radiation measurements made during overcast periods. Although roof and ground horizontal surfaces have similar radiating temperatures during these periods, vertical walls can still be warmer than surrounding surfaces. Note that at Casper, the walls were on the order of 2 °C warmer than roof and ground surfaces. Also, during the snow event at Colorado State University (CSU), the walls were on the order of 9 to 10 °C warmer than the snow-covered roof and ground surfaces.

Table 7. Surface radiating temperature measurements for cloudy cases. Temperatures in °C.

Station	Casper	Casper	CSU	CSU	CSU	Gaithersburg HS
Date/Time	1/18/1442	1/19/0740	2/9/1030	2/11/0930	2/11/1500	5/23/0715
Sky Condition	Overcast	Overcast	Overcast	Overcast, snowing	Overcast, snowing	Overcast
Roof SRT	8	-0.5	6.1	-6.7	-5.6	15
Roof material	White fabric	White fabric	Black rubber	Snow	Snow	Tar and gravel
Ground SRT	7.6	-1	5	-6.7	-5.6	15.6
Ground material	Grass	Grass	Grass	Snow	Snow	Grass
Wall SRT	10	1.8	5.6	2.2	3.9	15
Cloud Base SRT	-13.5		-15.6	-12.2		12.8
Concrete SRT	6.6	0.8		0.6		16.1
Asphalt SRT	7.8	1				16.7

3.1.2 Air temperature measurements

Air temperature measurements were made at two different sites during periods of overcast skies. The first site is Crest Hill Elementary School in Casper, WY.

Crest Hill Elementary School in Casper, WY is a single story roof. The roof surface is a white fabric and the existing sensor is mounted on a pole attached to the southeast corner of a secondary construction on top of the roof. The sensor is placed about 1.5 meters above the secondary roof (about a seven meter square building). The sensor is about six meters above the primary roof. The school is located on the outskirts of a suburban neighborhood in hilly terrain. Suburban housing developments surround the school on the north, south and east sides. To the west is a large North-South oriented

ridgeline and much less suburban development. The rooftop PRT was stationed within a foot of the existing sensor. The ground PRT was established on a five by eight meter grass plot to the east of the school. Sidewalks and parking lots surround the grass. The sensor was approximately seven meters from the east exterior wall of the school and approximately 65 meters from the rooftop sensor.

During the period of observation, 18-19 January 2000, the skies were overcast and winds were above 15 mph for the maximum readings but decreased to less than 10 mph for the minimum readings. The maximum air temperature recorded during the observation period was 8.7 °C while the low temperature was -1.1 °C.

The low overcast ceiling (approx. 9000 feet) should lead to small Q^* by making solar radiation (S) and downwelling longwave radiation ($L\downarrow$) of the same order. Small net radiation differences will lead to only small differences in sensible heat flux and air temperatures between roof and ground. Indeed, at the time of the maximum (1400-1600 MST), the roof SRT was 8 °C while the SRT of the grass was 7.6 °C (see Table 8). The concrete sidewalk surrounding the grass had an SRT of 6.6 °C, and the nearby parking lot's SRT was 7.8 °C. Both the roof and ground air temperatures were within 0.6 °C.

During the minimum (0700-0800 MST), the rooftop SRT of the white fabric was -0.5 °C while the grass was radiating at -1 °C. The roof and ground air temperatures recorded during this time were within 0.6 °C (See Figures 6 and 7). The small surface radiating temperature differences match with the small air temperature differences between roof and ground. These conditions are expected as the overcast skies should force net radiation small and minimize any horizontal differences in radiating temperatures. The similarity in surface radiating temperatures should drive the air

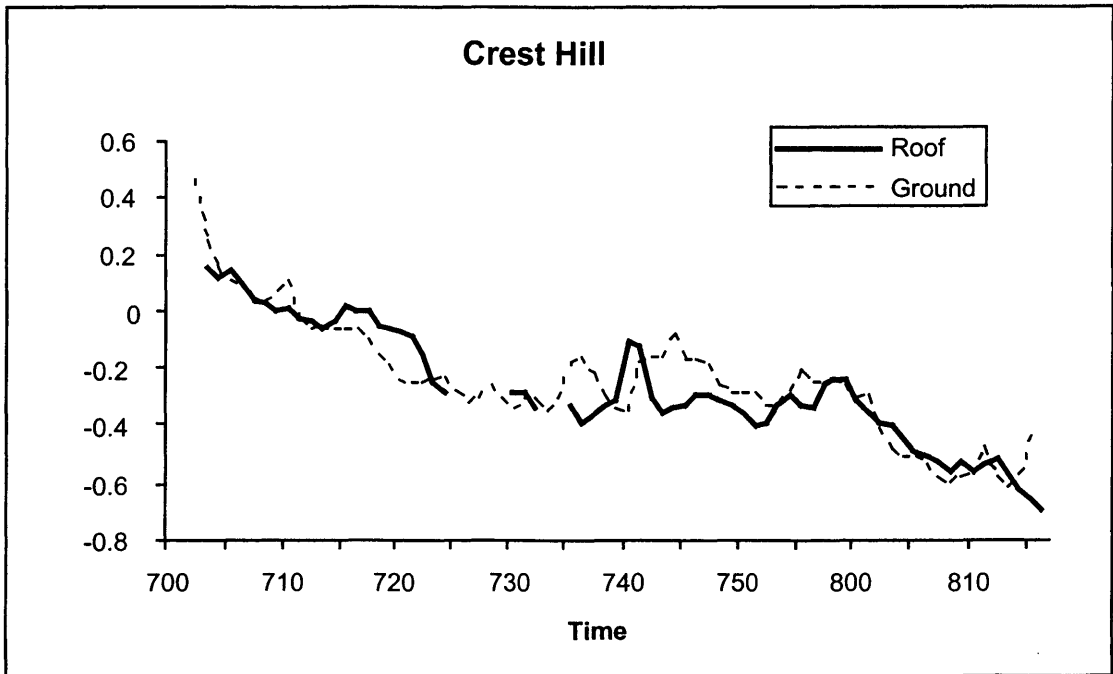


Figure 6. Crest Hill Elementary School air temperatures recorded by PRT on 19 January 2000.

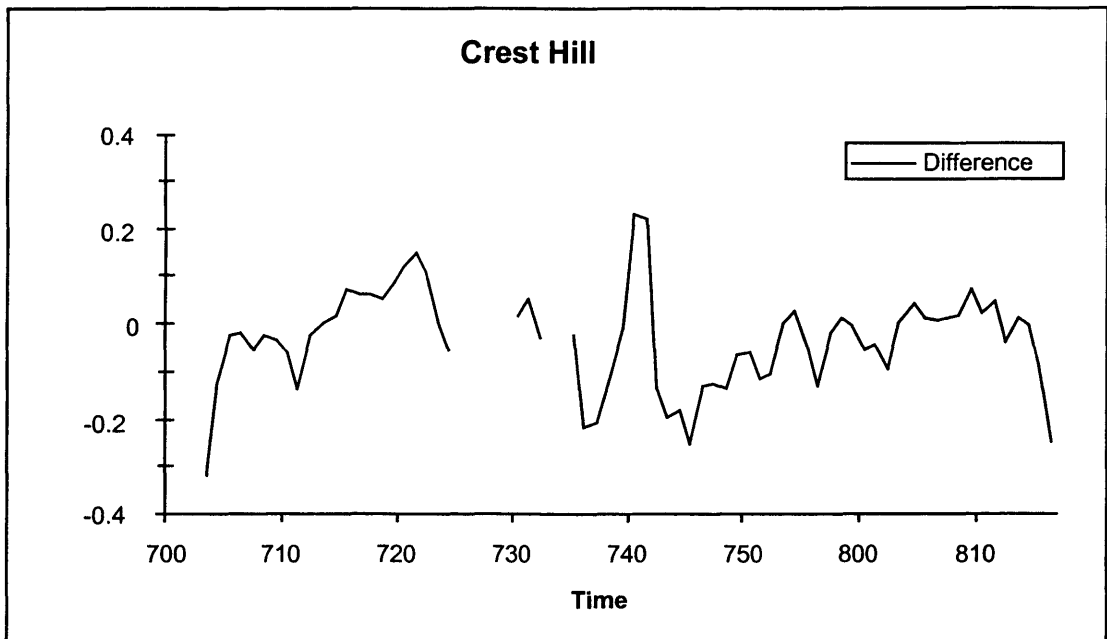


Figure 7. Crest Hill Elementary School air temperature differences (roof-ground) on 19 January 2000.

temperatures above the surfaces to be similar and the observations during this time support this assertion.

The next roof under observation was the Colorado State University Department of Atmospheric Science building. This roof is four stories high. A one meter high parapet surrounds it. The roof surface is black rubber sheeting. The RM Young PRT was placed at the southeast corner of the roof within 0.5 meters of the wall in order to simulate school weather stations mounted on a rod attached to an outside wall.

During this period, 9-15 February 2000, there was a significant snowfall event. It started to snow on the evening of the 10th and snowed through the night. By 11 Feb, there was a uniform two to three inch snow cover on the ground and the roof. It snowed lightly through the morning of the 11th but stopped by noon, keeping a thin overcast with light winds.

On the morning of the 11th, there was approximately a 1 degree C bias between roof and ground air temperatures. Through the day, the bias grew to a maximum of about 2.2 °C despite the thin overcast. However, note the rapid decrease in the temperature bias at sunset (See Figures 8 and 9). This indicates that the rooftop warm bias was a direct result of solar heating. But, the ground sensor was also exposed to the sun during the period. Why is there a difference between the two? The surface radiating temperatures on both the roof and the ground below the sensors were -5.6 °C. However, the south facing wall was radiating at 3.9 °C and the east facing wall at 2.2 °C. This data indicates that the snow covered surfaces had lower net radiation values due to high albedo while the south facing wall was able to absorb the radiation, leaving it with higher net radiation and thus greater sensible heat flux. The air in proximity to the wall warmed. As the air warmed it rose up the wall to finally bathe the rooftop PRT sensor in a rising plume of warm air. This is why the rooftop sensor showed anomalously high air temperature readings while

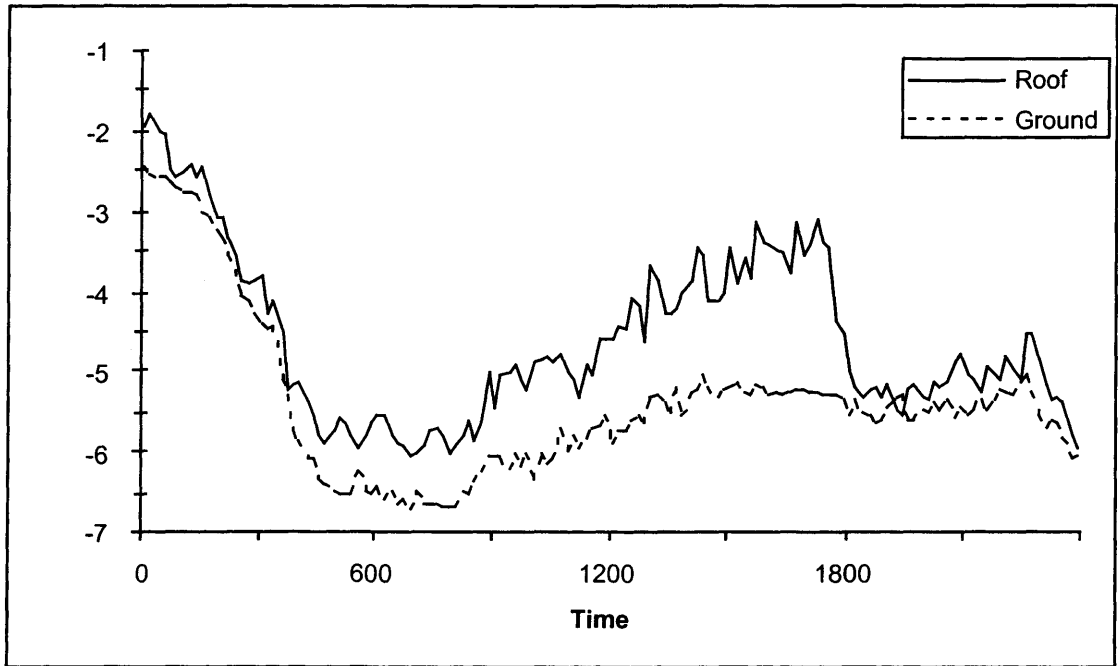


Figure 8. CSU Atmospheric Science Department air temperatures recorded by PRT on 11 February 2000. Wall effect case with uniform snow cover on both roof and ground.

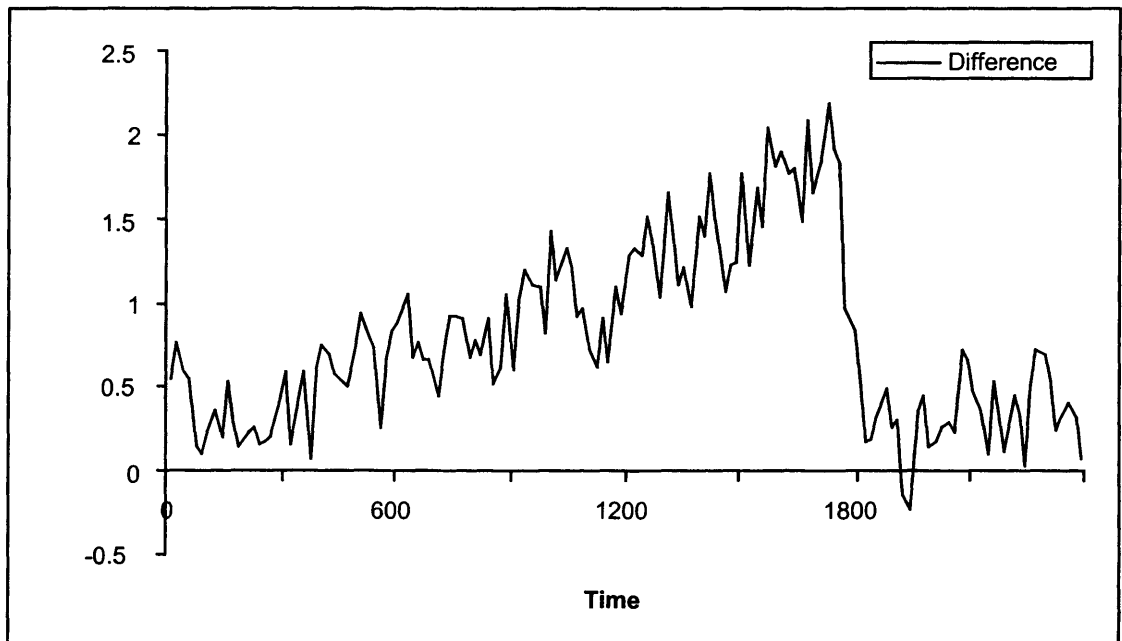


Figure 9. CSU Atmospheric Science Department air temperature differences (roof-ground) on 11 February 2000. Wall effect case.

both the roof and the ground surfaces were uniformly snow covered and radiating at the same temperature.

The most important result of this set of department observations was the dominant wall effect. During this day the surfaces beneath both roof and ground sensors were identical with uniform snow cover. The surfaces had the same radiating characteristics and were at the same temperature. However, the air sampled by the roof sensor was significantly warmer. The higher SRT of the wall indicates that the air was heated by the wall and then rose up the wall to the sensor. The wall effect should have a maximum on sunny winter days when sun angle is low and the sun-facing walls receive more radiation. This data shows that the wall effect can produce a significant difference even on cloudy days.

3.2 Clear Sky Cases

Rooftop versus ground scenarios should have minimal temperature differences when the skies are overcast. The radiation measurements in the previous section demonstrated that this is true in most radiating temperatures. The air temperature observations showed minimal differences at Crest Hill Elementary School but also showed an exceptional case of wall effect at CSU.

Clear sky cases should maximize any temperature bias that might exist at a rooftop site. By maximizing the incoming solar during the day, net radiation is increased and can lead to increased sensible heat flux from a surface to the air. The differences between a roof and ground surface can produce a daytime roof temperature bias. At night the clear skies allow for the most negative net radiation by maximizing surface radiative cooling to space. This leads to large negative sensible heat flux which, in turn, leads to more cooling above a surface.

3.2.1 Radiation Measurements

Radiation measurement during clear or partly cloudy sky periods were taken for several different rooftop sites. Table 8 demonstrates that radiation measurements taken during clear or partly cloudy periods show a wide variability. At Blevins Junior High School in Fort Collins, CO, the roof and ground were within one degree C at the time of the minimum. However, note that the temperature of the west wall of the building was on the order of 11 °C warmer than either roof or ground. The Meeteetse school in Meeteetse, WY showed the roof cooler than the ground at the time of the maximum. This could result from the albedo of the white fabric rooftop being greater than that of the surrounding grass. This could leave the roof with less net radiation and thus less sensible

Table 8. Surface radiating temperature measurements for clear / partly cloudy cases. Temperatures in degrees C.

Station	Blevins JHS, CO	Meeteetse, WY	Cody, WY	CSU	Asheville, NC	Kingsview MS, MD
Date/ Time	1/13/0650	1/19/1440	1/20/1430	2/1/1100	5/9/1220	5/24/1140
Sky Condition	Partly cloudy	Clear	Partly cloudy	Partly cloudy	Partly cloudy	Partly cloudy
Roof SRT	-12.1	-1.8	14	28	56.1	52.8
Roof material	Tar and gravel	White fabric	Tar and gravel	Black rubber	Tar and gravel	Shingle
Ground SRT	-13.1	6	9.5	14	38.9	25.6
Ground material	Grass	Grass	Grass	Sparse Grass	Concrete	Grass
Ground in shade			1.8	-3	21.1	20.6
Wall SRT	-1.8	12.5		21	36.7	
Concrete SRT		3.5	4.1		38.9	
Asphalt SRT		8.8		8	43.8	27.8
Other roof surface		-2.8 (snow)	4.5 (white fabric)	32 (black wall)	65.6 (tarpaper)	70 (metal)

heat flux to warm the air above. However, significant rooftop warm biases were observed at Cody, WY, Colorado State University, Asheville, NC, and Kingsview M.S., MD. The maximum temperature bias at these sites was 27 °C. There was a 45 °C difference between metal roofing and ground surface radiating temperatures at Kingsview Middle School, MD, but only a small fraction of the roof was metal. These large roof-ground surface radiating temperature differences certainly create large differences in sensible heat flux and should be reflected in the air temperatures.

3.2.2. Air Temperature Measurements

Air temperature measurements contrasting roof and ground were made at three separate sites during clear or partly cloudy periods. The first roof observed for this portion of the study was Blevins Junior High School in Fort Collins, CO. The second roof was the Cody police building in Cody, WY. The last roof observed during clear or partly cloudy skies was the CSU Atmospheric Science Department building.

Blevins Junior High School in Fort Collins, CO, is a one-story roof with two levels. The roof surface is tar and gravel and the existing sensor is mounted in the open, at least ten meters from any obstruction, on a tripod mast about three meters above the center of the roof surface. The school is located in a suburban neighborhood with suburban housing to the south, east and north and a large recreation field to the west. The RM Young PRT ground station was established over a grass plot off the southwest corner of the school approximately 20 meters from the school exterior wall and approximately 60 meters from the rooftop sensor. The PRT roof station was established directly adjacent to the existing rooftop sensor with the PRT sensor shield about 0.3 meters from the

existing radiation shield. There is a large parking lot about 30 meters west of the rooftop sensor and 30 meters north of the ground PRT.

During the period of observation on January 13, 2000, weather conditions were mild. Observations from the CSU campus weather stations two kilometers away reveal the sky was partly cloudy and temperatures ranged from a low of $-6.1\text{ }^{\circ}\text{C}$ at 0650hrs to a high of $14.9\text{ }^{\circ}\text{C}$ at 1530hrs. Winds remained under 10 mph for the entire period.

Measurements taken at the time of the minimum show differences on the order of $1\text{ }^{\circ}\text{C}$ between the roof and ground SRTs. The average surface temperature of the grass surrounding the ground-based sensor was $-13.1\text{ }^{\circ}\text{C}$. The roof's average SRT was $-12.1\text{ }^{\circ}\text{C}$. During this time, average air temperature measured by the rooftop PRT was $-5.1\text{ }^{\circ}\text{C}$ and the ground air temperature was $-6.3\text{ }^{\circ}\text{C}$ (See Figure 10). The average difference in air temperature between roof and ground was $1.2\text{ }^{\circ}\text{C}$ (See Figure 11).

A small difference was evident in the maximum temperature observations. The rooftop air temperature averaged $4.3\text{ }^{\circ}\text{C}$ for the hour from 1400-1500 MST. The average ground air temperature during this time was $3.9\text{ }^{\circ}\text{C}$ (See Figures 12 and 13). The small differences in surface radiating characteristics between roof and ground indicate there should be only small differences in air temperatures. The observations confirm this relationship.

Radiation observations of the school wall at the time of the minimum show the wall temperature was $-1.8\text{ }^{\circ}\text{C}$ compared to the grass at $-13.1\text{ }^{\circ}\text{C}$. During the time of the maximum, the west facing wall was $15.8\text{ }^{\circ}\text{C}$ while the grass was $7.8\text{ }^{\circ}\text{C}$. These measurements indicate the wall of the school is significantly warmer than the surrounding surfaces.

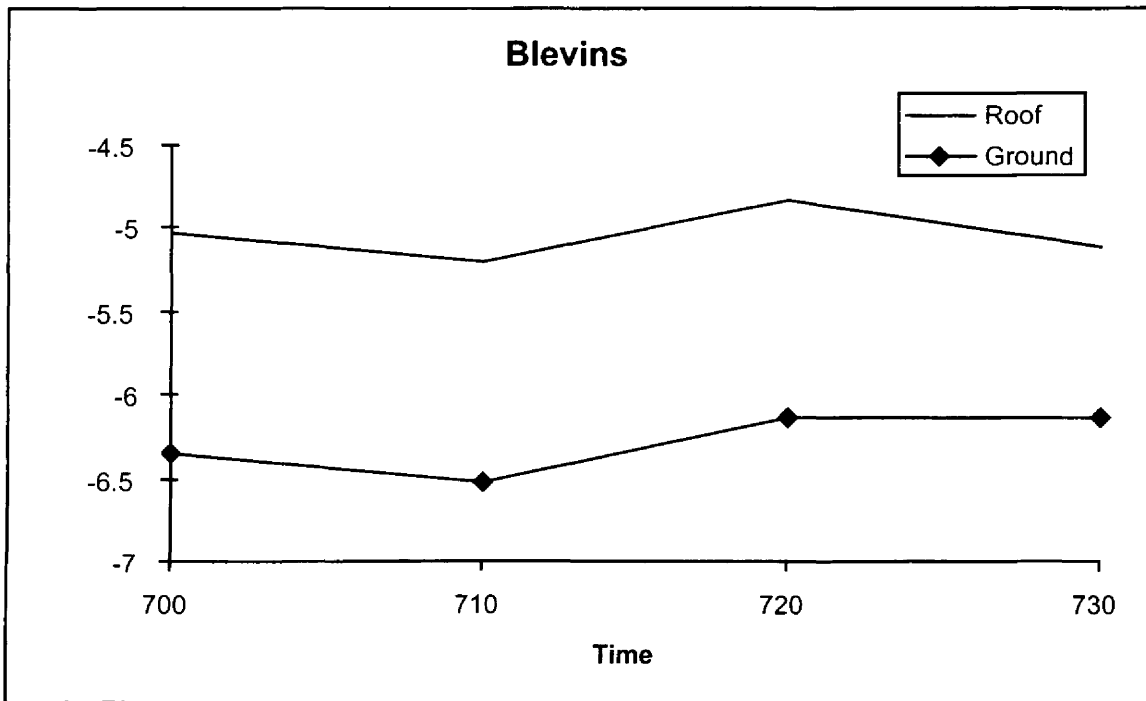


Figure 10. Blevins Junior High School morning air temperatures recorded by PRT for 13 January 2000.

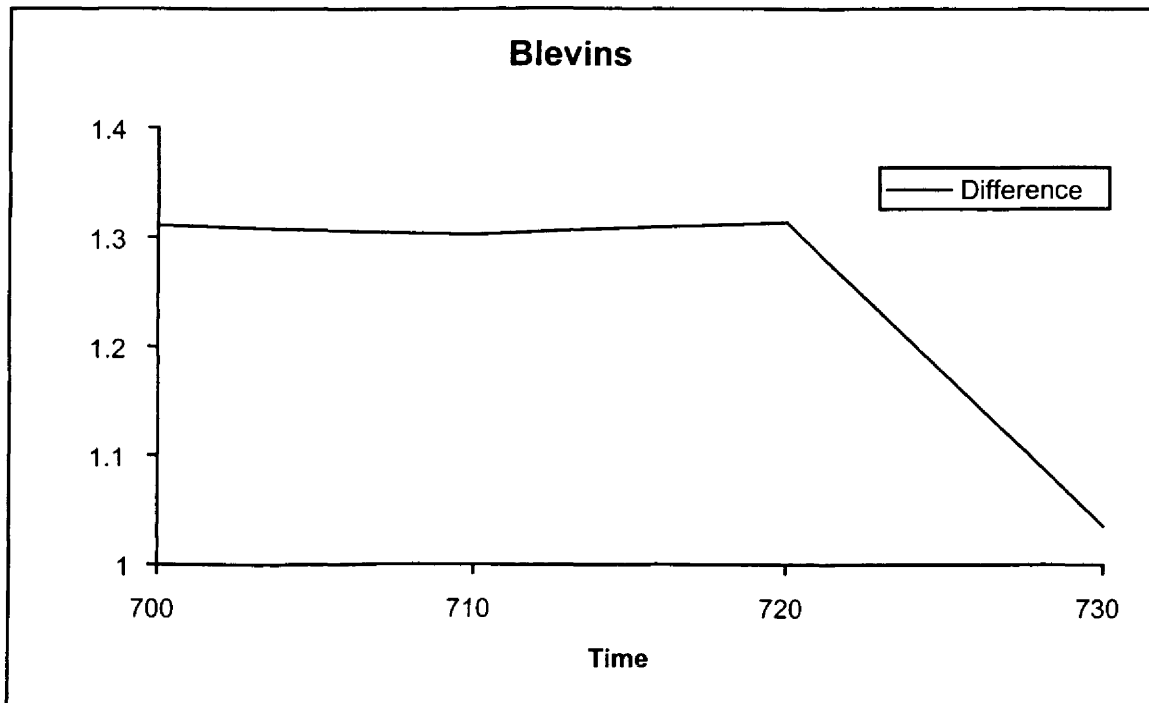


Figure 11. Blevins Junior High School morning air temperature differences (roof-ground) for 13 January 2000.

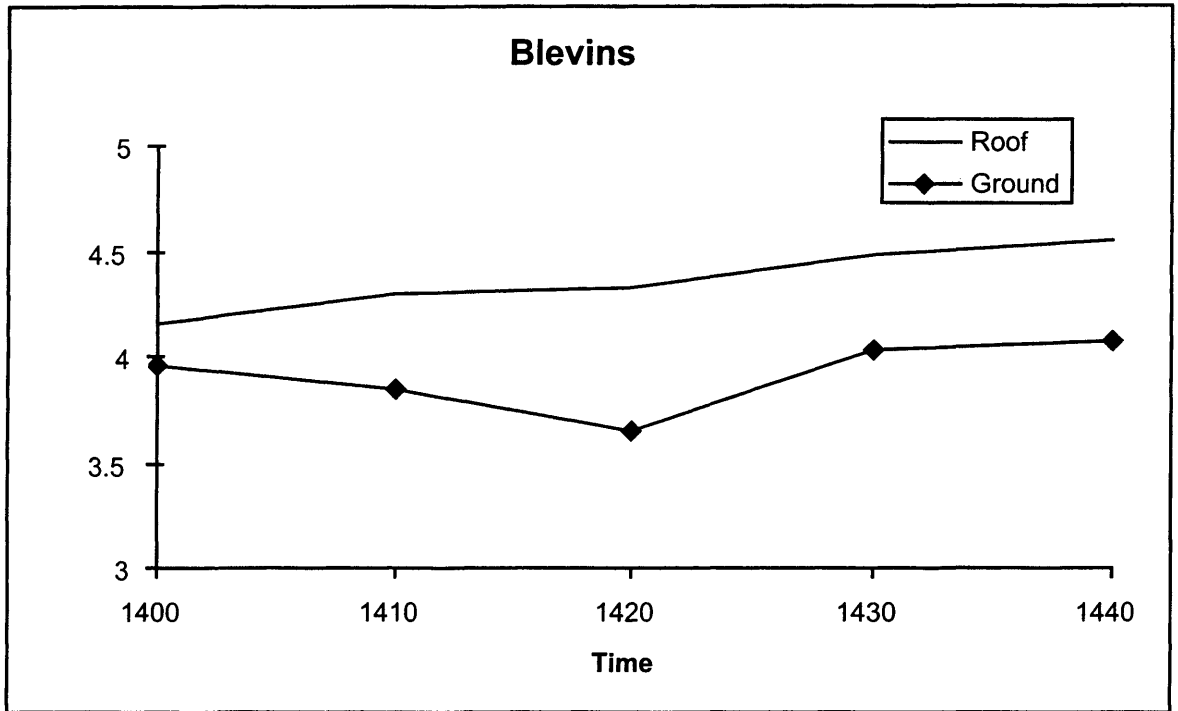


Figure 12. Blevins Junior High School afternoon air temperatures recorded by PRT for 13 January 2000.

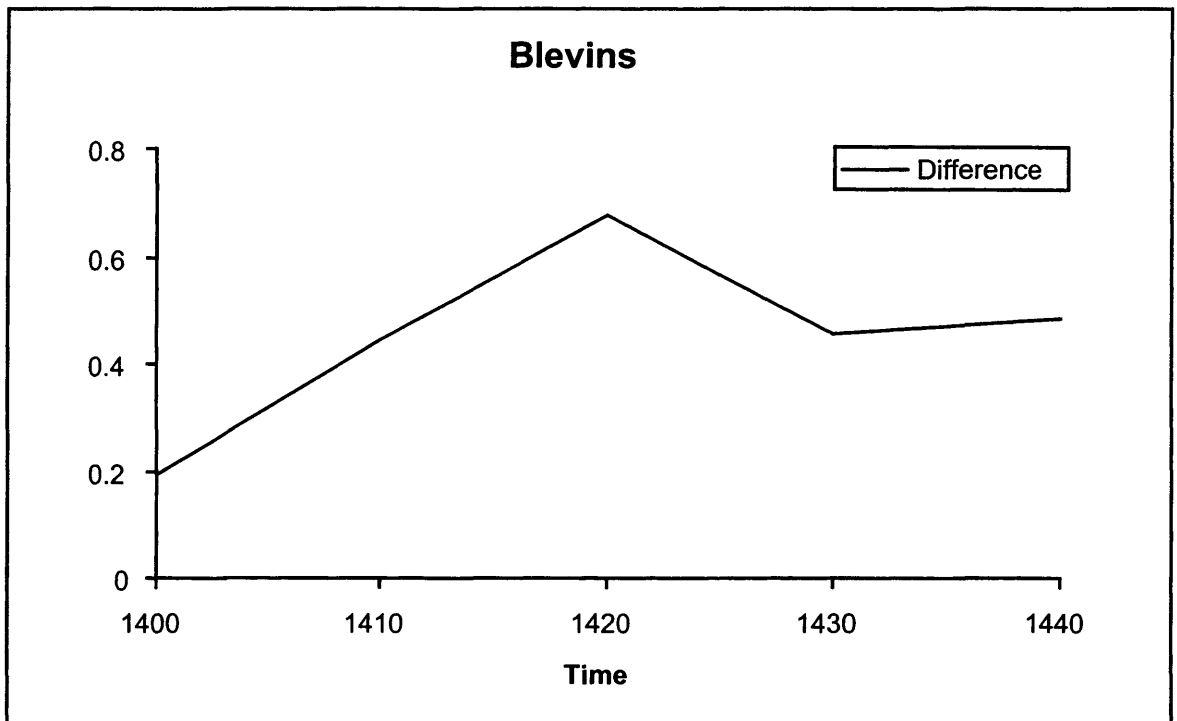


Figure 13. Blevins Junior High School afternoon air temperature differences (roof-ground) for 13 January 2000.

There was no evidence of a large rooftop bias at Blevins Junior High School. The differences in SRTs between roof and ground were on the order of 1 °C or less for both the maximum and minimum temperatures. In addition, the sensor is located away from obstructions in the middle of a large, one-story roof. The tar and gravel of the rooftop has an albedo of about 0.10 compared to the grass albedo of 0.16. These conditions and the observations indicate that this roof is probably representative of a nearby ground station.

The next station where air temperature measurements were made is the Cody police building. The Cody police building is a one-story building with multiple levels on the roof. The existing temperature sensor is located in a small wooden box about 1.5 meters above a tar and gravel roof surface. There are numerous exhaust vents on the roof including two different vents within three meters of the sensor. The sensor is located about two meters to the west of a three-foot high brick wall and about seven meters from the south edge of the building. The PRT ground sensor was placed about 70 meters north of the roof sensor over a snow covered open area. The ground PRT was approximately 13 meters from a building to the south and a building to the east. There was a major road located approximately 16 meters to the north of the sensor. The ground was covered in four-day old snow that was basically undisturbed except for the PRT apparatus itself. The snow was about four inches deep.

During the period of observation there was about four inches of snow on grass surfaces while the snow on paved surfaces had already melted off. All the snow on the roof had melted except for an approximately one inch layer of ice and snow that remained on a separate roof level. This roof surface was coated with a white vinyl material and was about one meter higher than the primary roof surface. Skies were

mostly cloudy during the afternoon but shifted to only partly cloudy by the next morning. Winds were below 10 mph for the afternoon but a warm downslope wind from the mountains to the west started between 1800 and 1900hrs. There was a corresponding jump in temperatures and these warm temperatures maintained during the night such that the maximum temperature of 6.6 °C occurred about 2330hrs. After approximately 0500hrs the winds decreased and the temperature dropped from 3.1 °C to the low temperature of -1.3 °C at 0700hrs.

For the short period where roof and ground observations were made, the PRT air temperatures were within 0.6 degree C (See Figures 14 and 15). During this time, surface radiating temperatures showed the tar and gravel under the sensor to be 14 °C while the nearby vertical brick wall was 25 °C. The white roof fabric had a SRT of 4.4 °C while the snow on the secondary roof had a SRT of -0.6 °C. The grass at the ground site had an SRT of 8.5 to 11 in the sun and 1.8 in the shade. The snow on the ground had an SRT of -1.8 °C.

The most interesting aspect of the Cody site was the retention of snow on the roof's white surface while not on the surrounding darker surfaces. The dependence on the emissivity of a surface is clearly evident in this case. The higher emissivity rooftop surfaces were snow free while the surface with a lower emissivity and higher albedo was still snow covered.

The next roof under observation was the Colorado State University Department of Atmospheric Science building. This roof is four stories high. A three-foot high parapet surrounds it. The roof surface is black rubber sheeting. The RM Young PRT was placed

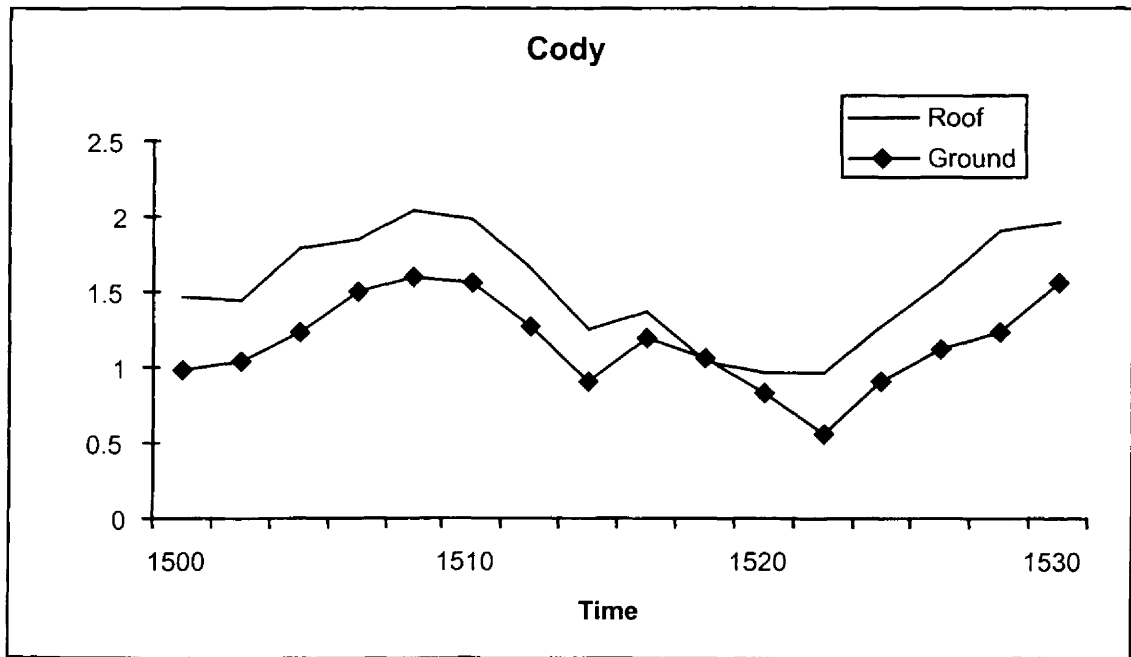


Figure 14. Cody Police Building air temperatures recorded by PRT on 20 January 2000.

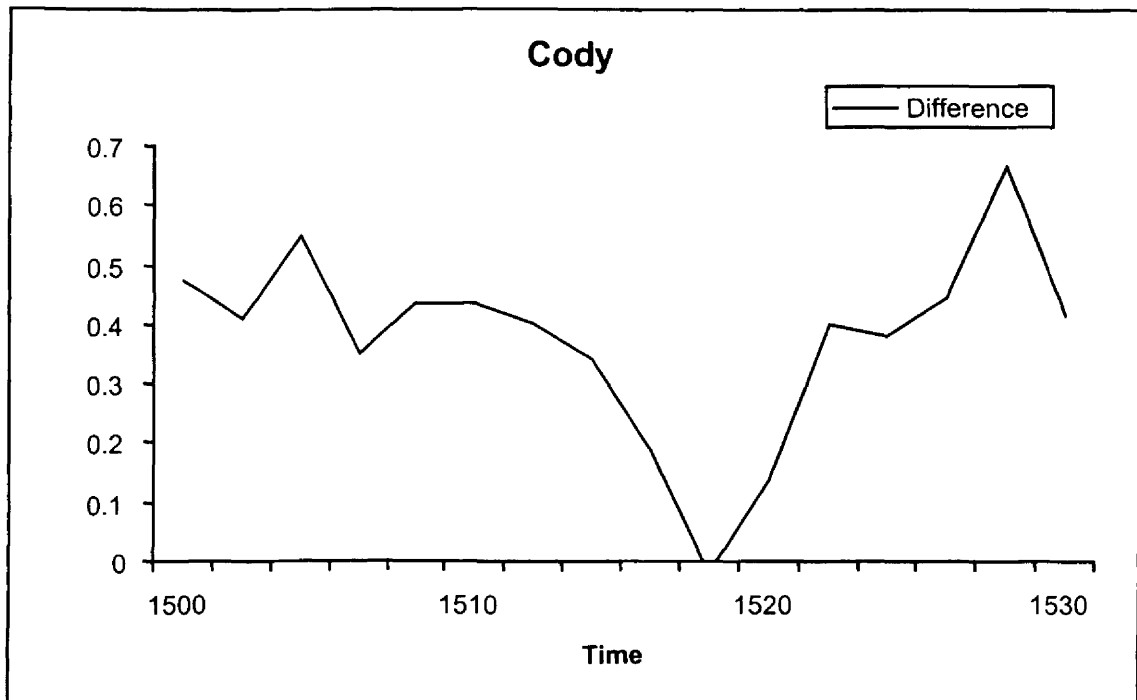


Figure 15. Cody Police Building air temperature differences (roof-ground) on 20 January 2000.

at the southeast corner of the roof within 0.5 meters of the wall in order to simulate school weather stations mounted on a rod attached to an outside wall.

During the first set of observations, a PRT was set up on a grass surface to the north of the building. The sensor was eight meters away from the exterior wall of the building and was in shade for the entire day except immediately after sunrise.

Conditions for the first series (28 Jan – 1 Feb 2000) were mostly cloudy for the first two days and then partly cloudy to clear after that.

The grass surrounding the PRT had a surface temperature of $-5\text{ }^{\circ}\text{C}$ in the shade and $14\text{ }^{\circ}\text{C}$ in the sun at 1100hrs on 1 February, 2000. During this same period, the black rubber roof had a surface radiating temperature of $28\text{ }^{\circ}\text{C}$. The PRT on the roof recorded a consistent warm bias of up to $2.8\text{ }^{\circ}\text{C}$ during this period (See Figures 16 and 17). The diurnal structure of the warm bias is evident in Figure 17. At the minimum, the rooftop and ground PRTs show fairly close agreement. They stay in agreement through the first part of the heating phase, but about halfway through the heating, the rooftop shows definite warming relative to the ground. By the maximum, the rooftop air temperature is clearly warmer than the ground air temperature each day of the period. About halfway through the cooling period, the temperatures converge with some differences still evident. By the time of the minimum, it appears that the air temperatures are much closer in agreement.

There clearly exists a warm bias in the Atmospheric Science Department Rooftop Temperatures. The rooftop is consistently warmer than the ground in both air and surface radiating temperatures during the maximum. This roof was expected to be warm because

of its low albedo (the black roofing material) and the location of the sensor in proximity to the wall and the warming associated with a wall effect.

An interesting aside to the measurements during this period arose with a comparison of the roof and ground air temperatures to that of a local automated weather station. The local site is approximately one kilometer from the department building but is about 22 meters lower. The department is on top of a hill and all the immediately surrounding terrain is lower. The co-op site is located on a level plain below the department. There is also a large ridgeline one kilometer to the west of the department.

The comparison between PRTs and the local site showed a pronounced cooling during the nighttime hours at the local site. The local site was on the order of 5 °C colder and up to 8.5 °C colder than either the ground or rooftop PRT. The local site is within 1 kilometer and might typically be considered to be representative of the temperatures for the local area. However, these measurements ask the question: what are the temperatures representative of?

During this period, three sensors were able to collect data. There was a rooftop PRT located over the south-facing wall, a ground PRT at the southeast corner of the building that received sun all day and a ground PRT north of the building that was in shade all day except immediately after sunrise. A comparison of the “north wall” shaded exposure with the full sun exposure reveals a median difference of 0.01 °C and a standard deviation in the difference of 0.6 °C

A third series of measurements was made at the CSU Atmospheric Science Department. This series consisted of two rooftop PRT sensors. The first PRT was located.

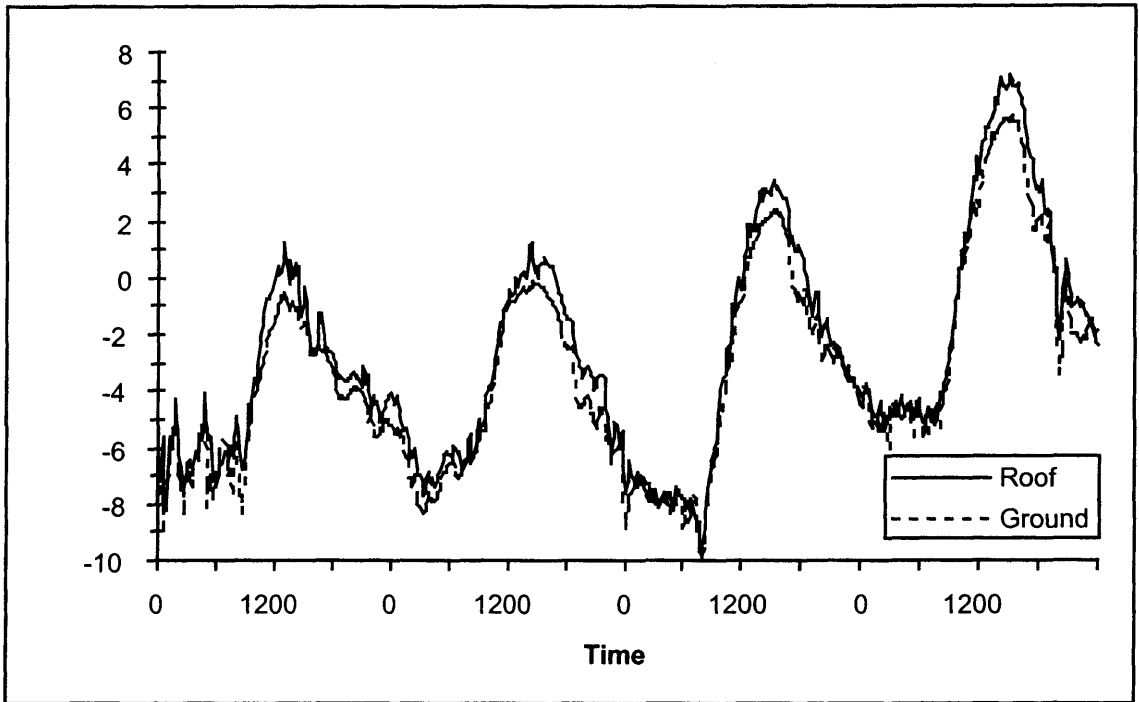


Figure 16. CSU Atmospheric Science Department air temperatures recorded by PRT for the period 29-31 January 2000.

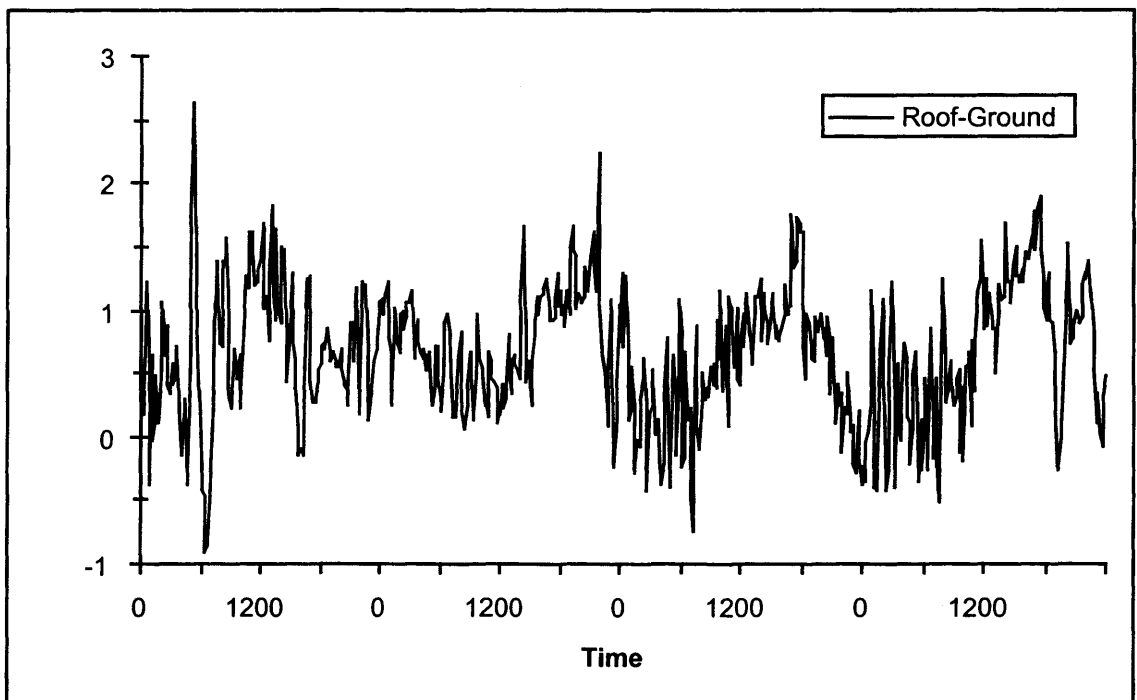


Figure 17. CSU Atmospheric Science Department air temperature differences (roof-ground) for the period 29-31 January 2000.

immediately over the south wall of the building while the second sensor was located towards the center of the rooftop. Both sensors were over the same black rubber sheeting but the first sensor was located to maximize any wall effect. The sensors were approximately ten meters apart

Observations taken during this period show that there is a warm bias in the sensor placed close to the wall during the maximum, coincident with south or east winds. The bias was on the order of 1 °C. Surface radiating temperatures made of the rubber sheeting during this time show that the roof surface under each sensor had the same SRT. The explanation for the difference between a “wall-mounted” sensor and a sensor in the center of the roof is a wall effect.

CONCLUSIONS

Rooftops can have significantly different temperatures than nearby ground stations. However, not all rooftops have a temperature bias. Rooftop temperature bias is caused by differences in surface characteristics. Rooftop bias can also vary seasonally and with weather conditions. Roofs can be warmer in both maximum and minimum temperatures, they can be neutral or they can be cooler in the maximum and perhaps the minimum. A rooftop sensor susceptible to a warm bias will have a low albedo roof surface, a restricted sky view, or be mounted on an exterior, sun-facing wall. A roof may also be warm when it is dry and the surrounding environment is wet through precipitation or irrigation. A representative rooftop sensor should also avoid any heat sources on the roof such as heating or air conditioning exhaust vents. Overcast skies or strong winds should eliminate any existing rooftop bias.

There was a wide variability in the rooftop exposures observed in this study. Clearly there is a need for standardization of rooftop exposures. The physical mechanisms for rooftop temperature bias can be exploited to develop a set of guidelines for acceptable exposures. Rooftops with high albedo and low emissivity should provide a good site. Sensors should be located away from heat sources such as exhaust vents. Sensors should also be located where they have a clear sky-view. Finally, sensors should be located away from exterior walls of building to avoid any wall effect. Sensor exposures that do not meet these standards may be subject to a rooftop temperature bias.

One way to survey a potential rooftop site for acceptability is to measure the surface radiating characteristics. Making measurements of the surface radiating temperature during the times of maximum and minimum temperature and comparing these SRTs to a “standard” site such as an open grass field enable the user to evaluate any tendency toward warm or cold bias. In addition to measuring the SRT of the surface beneath the exposure, the user can measure the SRT of the surrounding surfaces to detect any heat sources with the potential to warm the air. In addition, if the sensor is mounted to an exterior wall, the SRT measurements of the wall should indicate if the wall is warm relative to the surrounding ground surfaces and therefore has the potential to bias the sensor through a wall effect.

Finally, what is the measurement objective of the sensor? If the sensor is seeking to represent the air on top of the roof then it may not matter if the radiation and temperature characteristics of the rooftop differ from its surroundings. However, if the sensor is intended to represent the temperature of a large surrounding area, perhaps the radiation and temperature characteristics affecting the sensor should reflect those of the larger environment. This problem of representativeness is especially applicable to urban areas. Are urban surface materials and their inherent energy balance characteristics “unrepresentative” if the temperature sensor is to sample the environment people live in? This question of the intended use of a sensor’s data needs to be answered before the sensor exposure is established.

REFERENCES

- Armstrong, J.J., 1974: Temperature Differences Between Two Ground-Level Sites and a Roof Site in Southampton. *Meteorological Magazine*, **103**, 360-368.
- Arnfield, A.J., 1982: An approach to the estimation of the surface radiative properties and radiation budgets of cities. *Physical Geography*, **3**, 97-122.
- AWS, 1998: *AirWatch 4.5 Manual, PC Version*. Automated Weather Source, Inc., Gaithersburg, MD.
- Carlson, T.N., J.K. Dodd, S.G. Benjamin, and J.N. Cooper, 1981: Satellite estimation of the surface energy balance, moisture availability and thermal inertia. *Journal of Applied Meteorology*, **20**, 67-87.
- Dept. of Commerce, 1972: NWS Observing Handbook #2, Substation Operations. Dept. of Commerce.
- Geiger, R., 1966: *The Climate Near the Ground, Revised ed.*, Harvard University Press, Cambridge, MA, 611pp.
- Jones, C.A. and Ph.W. Suckling, 1983: Comparison of the Radiation Balance of a Rooftop Lawn with that of a Conventional Rooftop Surface. *Arch. Met. Geoph. Biocl.*, Ser. B, **33**, 77-87.
- Laskowski, B.R., 1936: Ground Temperatures Compared to Roof Temperatures. *Monthly Weather Review*, **64**, 17.
- Leffler, R.J. and J.W. Schiesl, 1994: Issues Concerning the Interpretation of Non-Standard Temperature Observations by national Weather Service Forecast Offices. National Weather Service.
- Meyer, S.J. and K.G. Hubbard, 1992: Nonfederal automated weather stations and networks in the United States and Canada: A preliminary survey. *Bull. Amer. Meteor. Soc.*, **73**, 449-457.
- Oke, T.R., 1978: *Boundary Layer Climates*, Halsted Press, New York, NY, 372pp.
- Oke, T.R., 1988: The Urban Energy Balance. *Progress in Physical Geography*, **12 (4)**, 471-490.

- Oke, T.R., G.T. Johnson, D.G Steyn, and I.D. Watson, 1991: Simulation of surface urban heat islands under 'ideal' conditions at night, Part 2: Diagnosis of causation. *Boundary-Layer Meteorology*, **56**, 339-358.
- Pielke, Roger A., 1984 : *Mesoscale Meteorological Modeling*, Academic Press, Orlando, FL.
- Robb, A.D., 1937: Comparison of Temperatures from Roof and Ground Exposures at Topeka, Kansas, 1935-36. *Monthly Weather Review*. Nov 1937, 388-392.
- Roth, M. and T.R. Oke, 1994: Comparison of Modelled and 'Measured' Heat Storage in Suburban Terrain. *Beitr. Phys. Atmosph.*, **67 (2)**, 149-156.
- WMO, 1996: *Guide to Meteorological Instruments and Methods of Observations*, 6th ed., World Meteorological Organization, Geneva.